Bull. Mater. Sci. (2022)45:89
https://doi.org/10.1007/s12034-021-02639-4

Formation of superhydrophobic porous GaAs layer: effect of substrate doping type

M NADDAF
Department of Chemistry, Atomic Energy Commission of Syria, P.O. Box 6091, Damascus, Syria
For correspondence (mnaddaf@aec.org.sy)

MS received 13 May 2021; accepted 20 November 2021

Abstract. In this report, the effect of the GaAs substrate type on the surface hydrophobicity of porous GaAs layers produced by an electrochemical etching method is investigated. At an etching time of 60 min, the porous GaAs layer formed on p^+-type GaAs substrate shows a hydrophobic surface with advancing water contact angle (θ_a) of around 140°, and a wetting hysteresis of ∼17.5°. Under the same equivalent etching conditions and parameters, the layer formed on n^+-type GaAs substrate exhibits self-cleaning superhydrophobic surface with advancing $\theta_a \approx 158°$, and a wetting hysteresis of ∼2.4°. This is attributed to doping type-induced morphological and structural modifications of porous GaAs layer, as it is inferred from scanning electron microscopy, atomic force microscopy, Raman scattering and X-ray photoelectron spectroscopy results and analysis. The layer formed on n^+-type substrate shows a β-Ga_2O_3-rich surface of micrometre-sized cone-like textures composed of bunched nano-wires, whereas the layer formed on p^+-type substrate exhibits an As_2O_3-rich micron-sized grooved structure. Superhydrophobic porous GaAs is of interest for prospective photovoltaic and sensing applications.

Keywords. Porous GaAs; superhydrophobic; SEM; AFM; Raman scattering; XPS.

1. Introduction

Due to their extreme repelling of water and self-cleaning behaviour, superhydrophobic surfaces have immense importance in many industrial, biological and biomedical applications [1–5]. These include their use as a biosensor platform, heat transfer surfaces and self-cleaning coatings for photovoltaic, greenhouse shields and medical devices [3–9]. Among many natural examples, the leaf of lotus rose is the most renowned one of the superhydrophobic surfaces with self-cleaning behaviour. It has been ascribed to joined effects of micro/nanostructure hierarchical structure (high roughness) and waxy nature (low energy) of its leaf surface that allow air to be trapped beneath the floating water drops [10]. This prevents the penetration of water into the surface and leads to the superhydrophobic and self-cleaning behaviour of the lotus leaf.

Owing to their low surface energy and high chemical stability, polymers are the most used materials for the artificial fabrication of the superhydrophobic surfaces and coatings. However, superhydrophobic surfaces produced on textured semiconducting and metallic substrates have attracted much attention from the scientific community, in the past two decades [11,12]. This is due to their capability for improving the performance of their bulk materials-based devices, as well as their potential for prospective novel applications.

Due to their simplicity, a wide range of parameters and comparatively low costs, chemical and electrochemical methods are among the most widely used methods for artificial fabrication of these surfaces [11–13]. A very important example is the superhydrophobic state on macroporous–nanoporous silicon films processed by electrochemical etching in HF-based electrolyte [13], or by a chemical etching combined with a chemical hydrophobization process [11,12]. These films have a very promising applications in microfluidic, bioanalytical, construction of high-efficiency and silicon-based solar cells with self-cleaning function [14]. However, the main disadvantage of porous silicon films is their lack of good chemical stability in atmospheric conditions.

The electrochemically etched surface of GaAs (porous GaAs) displays striking morphological, structural and optical properties of great importance from the applications point of view. It is demonstrated to be very promising material for photovoltaic, optoelectronic and bio-sensing applications [14–18]. Interestingly, its morphological, nature of chemical composition and nanostructuring properties can be highly altered by appropriate adjustments of its formation (etching) parameters. The influence of these parameters on morphological and structural properties of porous GaAs has been already reported [15–20]. However, the influence of these parameters on the wettability of the porous GaAs surface has not been yet addressed. This is an

Published online: 19 May 2022

important issue from application point of view of this material and justifies the experimental investigation addressed in this report. In particular, the realization of the superhydrophobic state on porous GaAs is desired for many of its applications. For example, porous GaAs with the self-cleaning surface is very attractive for prospective photovoltaic and sensing applications.

In the present report, it is demonstrated that by controlling the doping type of GaAs substrate, a highly stable superhydrophobic porous GaAs layer can be produced. The porous GaAs layer is formed by a pulsed electrochemical etching of highly doped <100> GaAs substrates in HF: HCl: C_2H_5 OH: H_2O_2:H_2O solution. The wetting properties of the produced layer are investigated by water contact angle (WCA) measurements and analysis. The morphological and structural properties of the layer are characterized by scanning electron microscopy (SEM), atomic force microscopy (AFM), Raman scattering spectroscopy and X-ray photoelectron spectroscopy (XPS). The wetting state of the produced layer could be transformed from hydrophobic to superhydrophobic, on using n^+-type GaAs substrate instead of p^+-type one, at a proper time of etching. This is attributed to the impact of the doping type of GaAs substrate on both morphological and structural properties of porous GaAs layer.

2. Experimental

Using the same procedures, electric source, electrolyte and etching cell, porous GaAs layers were formed by the pulsed electrochemical etching method described in previous report [16,19]. GaAs samples (1.5 cm × 1.5 cm) of both n^+-type <100> and p^+-type <100>, doped (1–7) × 10^{18} cm^{-3} with silicon and zinc, respectively, are used as substrates in this study. Using a Tektronix pulse generator, pulses with a pulse duration of 20 ms attained at a constant output voltage of 1.5 V were applied between the two electrodes of the cell. Under darkness, the etching time was varied from 20 to 60 min.

The produced porous GaAs layers were characterized using the same techniques of our previous reports [16,21]. The wetting properties of the produced layers were investigated by WCA measurements and analysis. The WCA measurements were carried out using contact angle measuring system OCA 15 plus from Data Physics Instrument GmbH. All measurements were carried out using a constant volume (3 µl) of distilled water droplets. For dynamic WCA measurements, the water droplet volume on the surface of the sample was advanced and receded, at a constant dispensing rate of 0.075 µl, and the wetting hysteresis was recorded as a function of the droplet age on the surface. A SEM from TESCAN was used to investigate the morphology of the porous GaAs layers. An AFM (AutoProbe CP-PSI) was used to estimate the average surface roughness of the porous GaAs layer. Raman spectra were recorded using a micro-Raman system HR 800 from Jobin Yvon-Horiba. Spectra were excited at room temperature using the 488 nm line of an argon laser source. The X-ray photoelectron spectroscopy (XPS) investigations were performed using a SPECS UHV/XPS/AES system with a hemispherical energy analyzer.

3. Results and discussion

The variation of the static WCA as a function of the etching time for porous GaAs layers formed on an n^+-type substrate (solid line) and p^+-type substrate (dotted line) is depicted in figure 1. In both cases, the WCA increases with increasing the time of etching and reaching a maximum value for etching time of 60 min. However, the increase in the value of WCA is notably higher in the case of the layer formed on an n^+-type substrate. This indicates that under the same etching parameters, the doping type of the GaAs substrate has a high impact on the wettability of the produced porous GaAs layer. In particular, the layer formed on an n^+-type substrate reaches a superhydrophobic state at an etching time of 60 min. It is expected that the surface roughness of the porous semiconducting materials increases with increasing of the electrochemical etching time [22]. However, it has been reported that the morphology of porous GaAs suffers a kind of destruction at a prolonged time of etching [16]. This may explain the observed decrease in the WCA for the layer produced at an etching time of 75 min.

Figure 2 shows the dynamic change of the WCA on the surface of the porous GaAs layer formed at the etching time of 60 min on (a) n^+-type GaAs substrate and (b) p^+-type GaAs substrate. The values of advancing contact angle (θ_a) are around 158° and 140° for the layer formed on n^+-type and p^+-type substrates, respectively. Whereas, the corresponding values of receding contact angle (θ_c) are around 155.6° and 122.5°, respectively. These correspond to a wetting hysteresis (θ_a–θ_c) of around 2.4° and 17.5°,

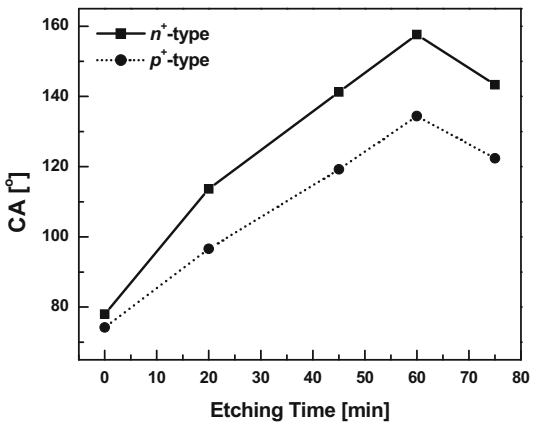

Figure 1. Variation of static WCA as a function of etching time for porous GaAs layers formed on and n^+-type substrate (solid line) and p^+-type substrate (dotted line).

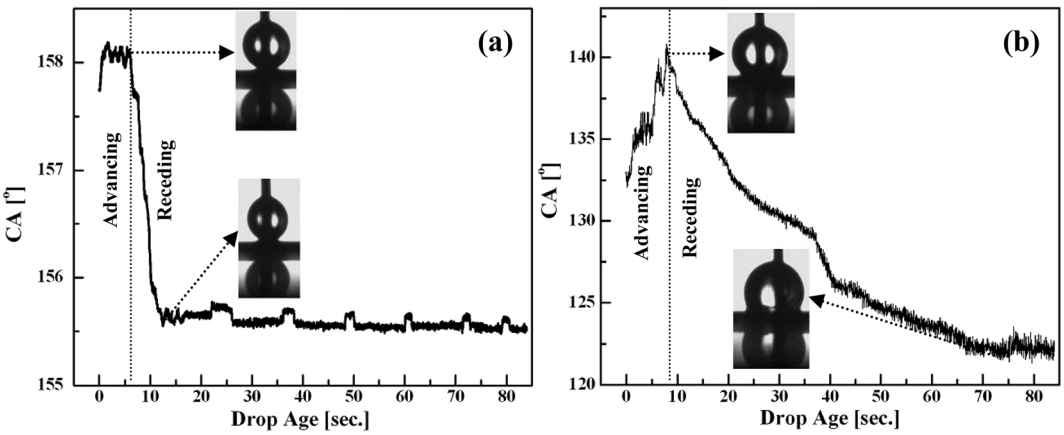

Figure 2. Dynamic change of the WCA on the surface of the porous GaAs layer formed at the etching time of 60 min on: (**a**) n^+-type GaAs substrate and (**b**) p^+-type GaAs substrate. The insets show the images of the water droplet, as it is advanced (top), and receded (bottom) on the surface of each of the two samples.

respectively. Moreover, as it can be seen from figure 3 that on tilting the porous GaAs layer formed on n^+-type concerning to its horizontal position, the water droplet rapidly rolls off the surface and settles down on the un-etched part of the GaAs. This non-wetting behaviour indicates that this layer has a self-cleaning property. In order to assert this conclusion, a silica powder was rested on this sample and a water droplet was then syringed over its tilted surface [23]. As it can be observed from figure 4, the water droplet picks the silica powder along its rolling path. This indicates that this layer has a self-cleaning property. More importantly, this layer has shown high stability in this property as a function of ageing time. It has preserved its superhydrophobic nature, even after ageing it at the laboratory conditions for more than 2 years. As compared to the superhydrophobic surfaces of polymeric materials [24,25], the produced porous GaAs layer does not suffer from any hydrophobic recovery and has much better durability under water and ambient conditions.

Many factors, such as chemical constitution, surface roughness and molecular packing affects the value of a liquid contact angle. Hence for a given material, the contact

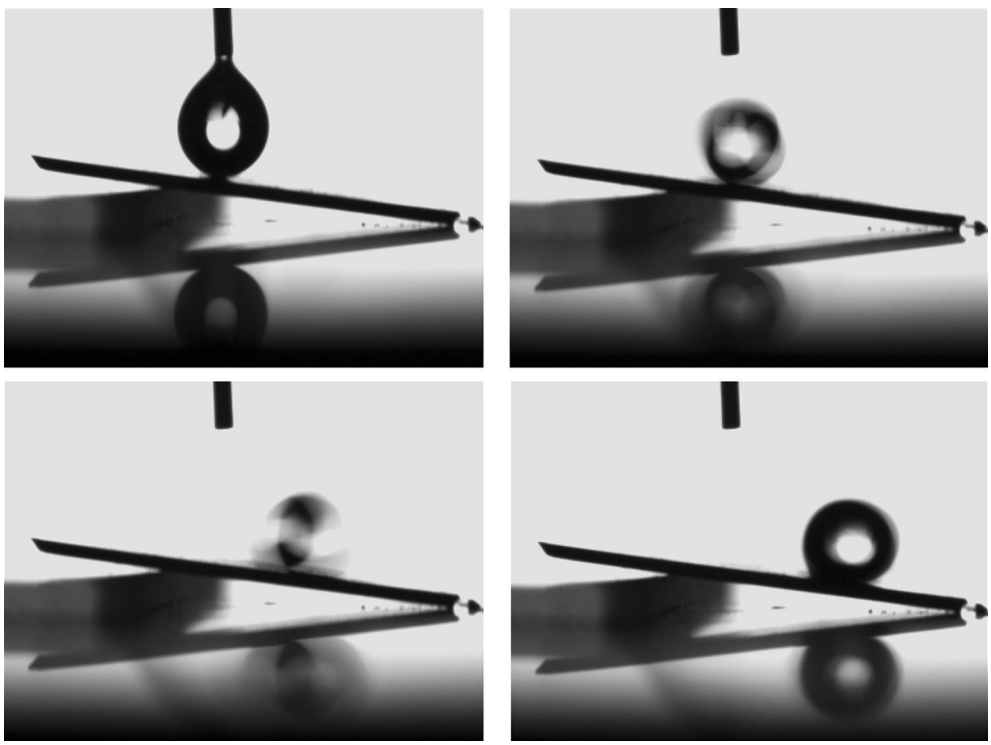

Figure 3. Four consecutive images exhibiting the water droplet as it is rolling off the tilted porous GaAs sample formed on n^+-type GaAs substrate at etching time of 60 min.

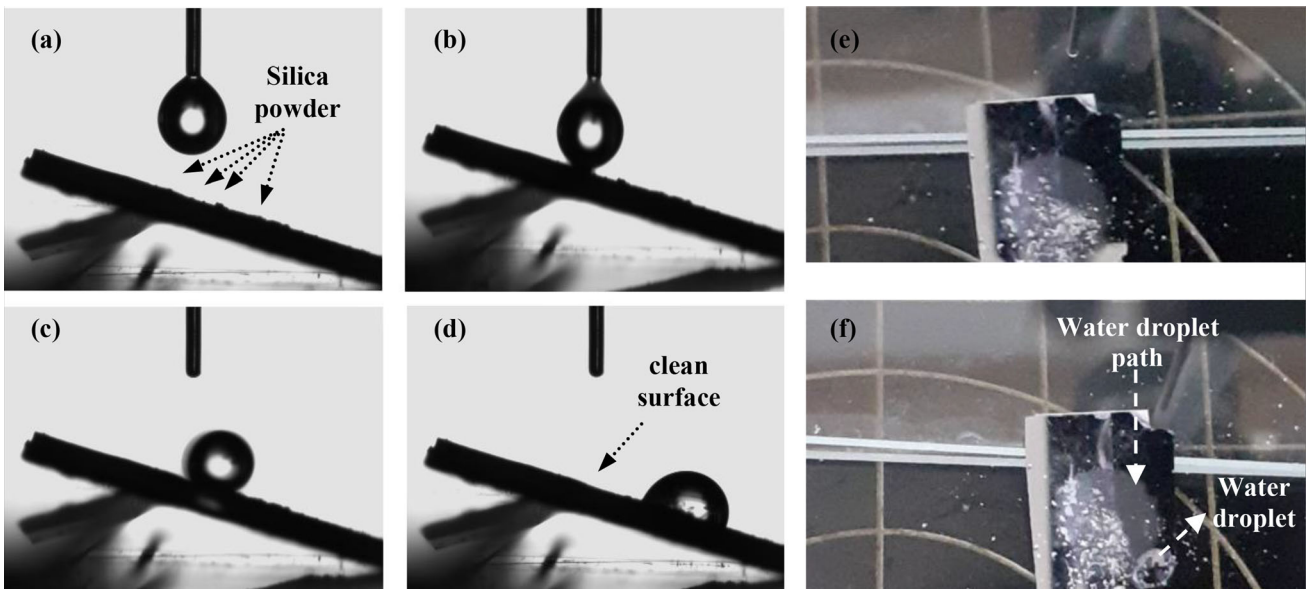

Figure 4. Demonstration of self-cleaning properties of porous GaAs sample formed on n^+-type GaAs substrate: (**a–d**) selected images before, during and after syringing the water droplet on its silica powder-contaminated surface, (**e**) and (**f**) camera photos of this sample before and after the rolling process of the water droplet.

angle value is determined by the collective effect of these factors. The influence of doping type on the morphological aspects and the surface chemistry of the porous GaAs layer produced at etching time of 60 min, was investigated using SEM, AFM, Raman scattering and XPS techniques.

Figure 5 shows SEM micrographs of the porous layers formed on GaAs substrate of (a) p^+-type and (b) n^+-type. The layer formed on p^+-type substrate exhibits a macro-porous structure composed of micron-sized grooved-like textures. However, the porous GaAs layer formed on n^+-type substrate shows a hierarchical structure of cone-like features of micron size that is composed of bunched nano-wires. In addition, it is clear from these images that the layer formed on n^+-GaAs substrate has higher surface roughness than the one formed on p^+-GaAs substrate. To confirm this, the SEM results were further assisted by AFM images. It is observed from the AFM images in figure 6 that similar to SEM results, the layer formed on p^+-type substrate exhibits corrugated grooved structures, while the one formed on n^+-type shows a hierarchical structure consisting of micro-size features composed of bunched wires, and nano-size porous structures. Using line profile analysis of

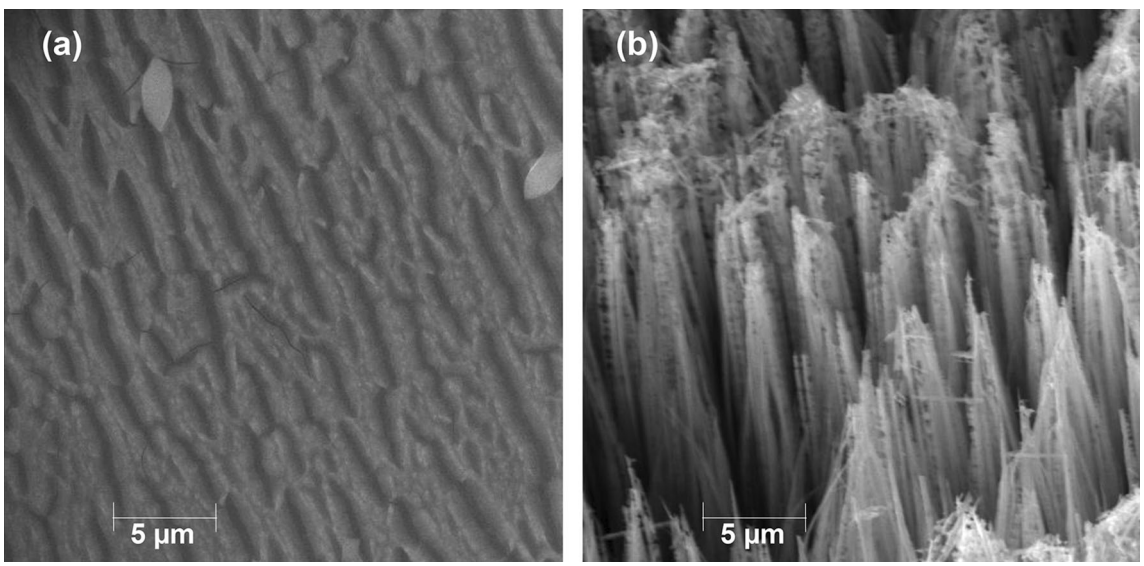

Figure 5. SEM micrographs of porous GaAs layers formed at etching time of 60 min on GaAs substrate of: (**a**) p^+-type and (**b**) n^+-type.

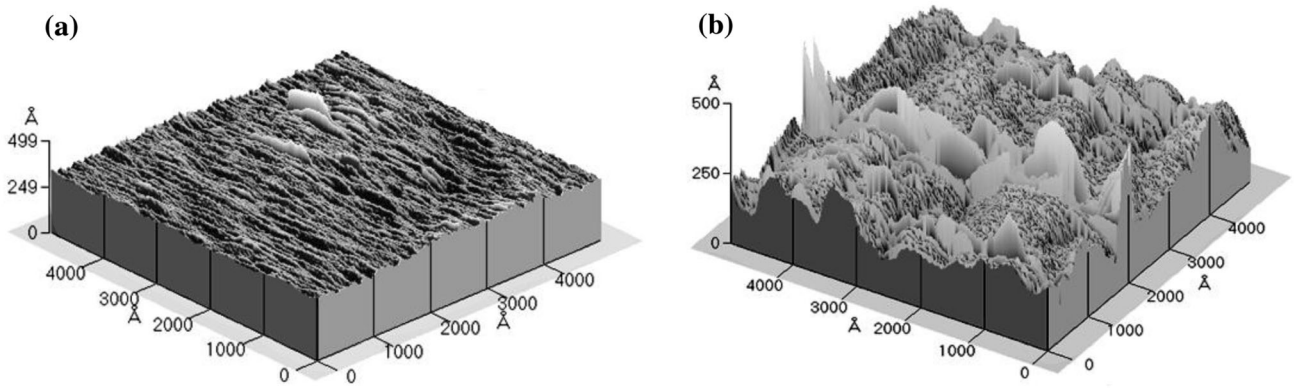

Figure 6. Three-dimensional-AFM images of porous GaAs layers formed at etching time of 60 min on GaAs substrate of: (**a**) p^+-type and (**b**) n^+-type.

the 2-D AFM images of these samples, the value of average surface roughness value (R_a) is ∼1.48 and ∼5.79 nm, for the layer formed on p^+-type substrate and on n^+-type substrate, respectively.

In the previous reports of our group, the Raman spectra of porous GaAs were formed on p^+-type and n^+-type GaAs substrates under similar etching conditions and parameters, but by applying an output pulse of 1 V instead 1.5 V in this report [16,19]. Similar spectral features of previously reported Raman results is also observed in the present case, as it is shown in figure 7. It can be seen that the Raman spectrum of the sample formed on p^+-type shows several sharp Raman lines that typically correspond to As_2O_3 (arsenolite) [20]. In addition to the Raman lines due to GaAs nanocrystals and defect arsenic vacancy [16,19,26,27], the Raman spectrum of the sample formed on n^+-type shows a strong and broad peak related to β-Ga_2O_3 (claudetite) [28].

Figure 8 shows the high-resolution XPS peaks of arsenic As_{3d} levels for the porous GaAs layer formed on (a) p^+-type GaAs substrate and (b) n^+-type GaAs substrate. In both cases, the spectrum of As_{3d} level shows two peaks; the low

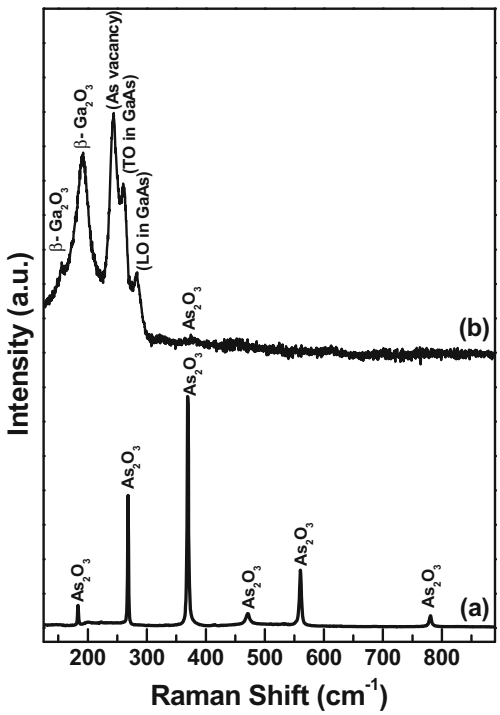

Figure 7. Raman spectra of porous GaAs layers formed at etching time of 60 min on GaAs substrate of: (**a**) p^+-type and (**b**) n^+-type.

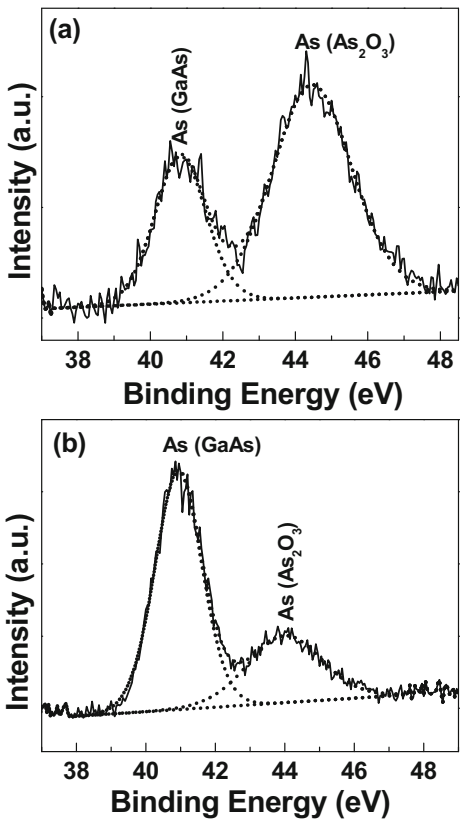

Figure 8. X-ray photoelectron spectra of As_{3d} for GaAs layers formed on: (**a**) p^+-type GaAs substrate and (**b**) n^+-type GaAs substrate.

binding energy peak corresponds to As in GaAs (As_{nox}) and the high binding energy one associates with arsenic trioxide As_2O_3 (As_{ox}). However, the at% ratio (As_{ox}/As_{nox}) is found from these spectra to be around 2.23 and 0.45 for p^+-type and n^+-type, respectively. Figure 9 shows the high-resolution XPS peaks of gallium Ga_{3d} levels for porous GaAs layer formed on (a) p^+-type GaAs substrate and (b) n^+-type GaAs substrate. The Ga_{3d} peak in both cases is deconvoluted into two components (dot lines); the low binding energy peak corresponds to Ga in GaAs (Ga_{nox}) and the high binding energy assigns to Ga in Ga_2O_3 (Ga_{ox}). The ratio of Ga_{ox}/Ga_{nox} is found to be around 0.36 and 3.6 for p^+-type and n^+-type, respectively.

The above XPS and Raman results indicate that the porous layer formed p^+-type substrate is As_2O_3-passivated, while the one formed on n^+-type substrate is Ga_2O_3-rich. Since oxides-rich surfaces are generally hydrophilic, it can be deduced from the above AFM results that the surface roughness plays the dominant role in determining the value of WCA of the formed layers. The layer formed on n^+-GaAs substrate shows higher surface roughness than the layer formed on p^+-GaAs substrate. It is well established that as the surface roughness increases, the contact angle increases due to the increase in the fraction of air trapped under the water droplet, which in turn prevents the penetration of water into the surface. The fraction of trapped air can be estimated according to Cassie and Baxter theory [29,30], using the following equation [29]:

$$\cos\theta_{CB} = f_s\cos\theta - f_a, \quad (1)$$

where θ_{CB} is the apparent CA of a drop of liquid (water in our case), on the rough surface (porous GaAs layer), θ is the CA of a drop of liquid on the flat solid surface (GaAs substrate), f_s and f_a are the fractional interfacial areas of solid and air on the surface, respectively, and $f_s + f_a = 1$. The values of WCA for p^+-GaAs substrate and n^+-GaAs substrate are seen from figure 1 to be around 74.2° and 78°, respectively. From the above equation and the experimental data in figure 1, the value of f_a is found to be around 0.77 and 0.928 for porous GaAs layers prepared at an etching time of 60 min on p^+-GaAs substrate and n^+-GaAs substrate, respectively. This means that for n^+-type GaAs substrate, 92.8% of the water droplet contacts the trapped air, while only 7.2% contacts the real surface of the layer. Hence, due to the high roughness of the hierarchical structure of the porous layer formed on n^+-type GaAs substrate, the fraction of the air trapped under the water droplet greatly increases, and thus preventing the penetration of the water into its surface. Since the porous layer formed on p^+-type GaAs substrate shows high values of both WCA and wetting hysteresis, it is also of importance to note that similar to that of rose petal, the wetting state of this sample is more likely to follow the Cassie impregnating wetting state on the unevenly rough surface [31].

Moreover, Gao *et al* [32] demonstrated that β-Ga_2O_3 nano-wire film prepared on porous GaP substrate can attain a superhydrophobic state. In the present report, the Raman results show that the porous layer formed on n^+-GaAs substrate has β-Ga_2O_3-rich surface. Hence, the observed conversion from hydrophobic for p^+-type GaAs to superhydrophobic state for n^+-type GaAs can be attributed to the contribution of the doping type effect on both morphological and chemical structural properties of porous GaAs layer.

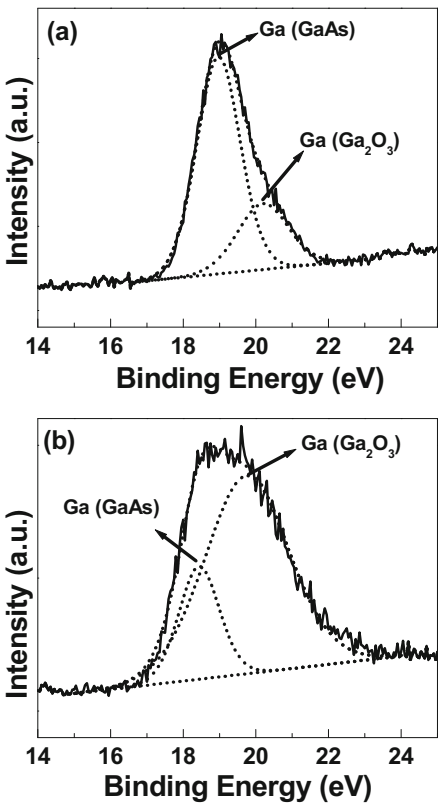

Figure 9. X-ray photoelectron spectra of Ga_{3d} for GaAs layers formed on: (**a**) p^+-type GaAs substrate and (**b**) n^+-type GaAs substrate.

4. Conclusion

Porous GaAs layers have been produced on electrochemically anodized both p^+-type and n^+-type GaAs substrates in a HF:HCl:C_2H_5OH: H_2O_2:H_2O electrolyte. The doping type of GaAs substrate is found to have a significant impact on the morphology and the nature of oxides of the formed porous GaAs layers, which importantly affected the wetting properties of the layer. Under the same equivalent etching conditions, WCA measurements show that the layer formed p^+-type substrate exhibits a hydrophobic surface, while the layer formed n^+-type substrate shows a highly stable roll-off superhydrophobic surface with contact angle hysteresis of around 2.4°. Fabrication of superhydrophobic porous GaAs layer with self-cleaning properties and excellent

durability under water and ambient conditions is of particular importance for GaAs-based photovoltaic and sensing applications.

Acknowledgements

We would like to acknowledge Prof. I Othman, the Director General of AECS, and Prof. N Mir-Ali, the Head of Molecular Biology and Biotechnology Department, for their support.

References

[1] Parvate S, Dixit P and Chattopadhyay S 2020 *J. Phys. Chem. B* **124** 1323
[2] Feng L, Li S, Li Y, Li H, Zhang L, Zhai J, *et al* 2002 *Adv. Mater.* **14** 1857
[3] Shirtcliffe N J, McHale G, Atherton S and Newton M I 2010 *Adv. Colloid Interface Sci.* **161** 124
[4] Ma M and Hill R M 2006 *Curr. Opin. Colloid Interface Sci.* **11** 193
[5] Latthe S S, Terashima C, Nakata K and Fujishima A 2014 *Molecules* **19** 4256
[6] De Angelis F, Gentile F, Mecarini F, Das G, Moretti M, Candeloro P, *et al* 2011 *Nat. Photon.* **5** 682
[7] Wu X H, Liew Y K, Mai C-W and Then Y Y 2021 *Int. J. Mol. Sci.* **22** 3341
[8] Jokinen V, Kankuri E, Hoshian S, Franssila S and Ras R H 2018 *Adv. Mater.* **30** 1870173
[9] Chenab K K, Sohrabi B and Rahmanzadeh A 2019 *Biomater. Sci.* **7** 3110
[10] Barthlott W and Neinhuis C 1997 *Planta* **202** 1
[11] Cao M, Song X, Zhai J, Wang J and Wang Y 2006 *J. Phys. Chem. B* **110** 13072
[12] Wang F, Zhao K, Cheng J and Zhang J 2011 *Appl. Surf. Sci.* **257** 2752
[13] Ressine A, Finnskog D, Marko-Varga G and Laurell T 2008 *Nanobiotechnology* **4** 18
[14] Ressine A, Marko-Varga G and Laurell T 2007 *Biotechnol. Annu.* **13** 149
[15] Föll H, Carstensen J and Frey S 2006 *J. Nanomater.* **2006** ID 091635
[16] Naddaf M and Saad M 2013 *J. Mater. Sci. Mater. Electron.* **24** 2254
[17] Tondare V, Naddaf M, Bhise A, Bhoraskar S, Joag D, Mandale A, *et al* 2002 *Appl. Phys. Lett.* **80** 1085
[18] Duplan V, Frost E and Dubowski J J 2011 *Sensor Actuat. B-Chem.* **160** 46
[19] Naddaf M 2017 *J. Mater. Sci. Mater. Electron.* **28** 16818
[20] Lockwood D, Schmuki P, Labbe H and Fraser J 1999 *Physica E Low Dimens. Syst. Nanostruct.* **4** 102
[21] Naddaf M and Alkhawwam A 2016 *Diam. Relat. Mater.* **64** 57
[22] Naddaf M, Awad F and Soukeih M 2007 *Mat. Sci. Eng. C* **27** 832
[23] Banik M, Chakrabarty P, Das A, Ray S K and Mukherjee R 2019 *Adv. Mater. Interfaces* **6** 1900063
[24] Bhandaru N, Agrawal N, Banik M, Mukherjee R and Sharma A 2020 *Bull. Mater. Sci.* **43** 1
[25] Varughese S M and Bhandaru N 2020 *Soft Matter* **16** 1692
[26] Tiginyanu I, Irmer G, Monecke J, Vogt A and Hartnagel H 1997 *Semicond. Sci. Technol.* **12** 491
[27] Berg R and Yu P 1987 *Phys. Rev. B* **35** 2205
[28] Gao Y, Bando Y, Sato T, Zhang Y and Gao X 2002 *Appl. Phys. Lett.* **81** 2267
[29] Cassie A and Baxter S 1944 *Trans. Faraday Soc.* **40** 546
[30] Cassie A 1948 *Discuss. Faraday Soc.* **3** 11
[31] Ghosh U U, Nair S, Das A, Mukherjee R and DasGupta S 2019 *Colloids Surf. A Physicochem. Eng. Asp.* **561** 9
[32] Gao L, Zheng M, Zhong M, Li M and Ma L 2007 *Appl. Phys. Lett.* **91** 013101